Journal of Civil Engineering (IEB), 36 (1) (2008) 43-63

Journal of Civil Engineering IEB

Analysis of local bending in twin-wall pipes: comparison with measurements

Ashutosh S. Dhar[1] and Ian D. Moore[2]

[1]*Department of Civil Engineering*
Bangladesh University of Engineering Technology, Dhaka 1000, Bangladesh
[2]*Department of Civil Engineering, Queen's University, Kingston ON, Canada*

Received 2 January 2008

Abstract

Profiled pipes of thermoplastic materials have been used increasingly as underground conduit for transporting water and waste water. Pipes of different sizes (diameters ranging 450 mm to 2400 mm for High Density PolyEthylene Pipe) with a wide variety of wall geometries have been developed to obtain higher wall stiffness with less utilization of material. The shapes of those profiles often cause localized deformations which may govern the performance of the pipes. An investigation of the localized deformation (local bending) on two different profile-wall HDPE pipes is presented in this paper. Axisymmetric finite element analysis was used to study the profile responses under axisymmetric loading. A semi-analytical finite element method, based on axisymmetric idealization of the profile, was employed to study the profile behavior in a more realistic (biaxial) stress field expected for a pipe buried horizontally in the ground. The result of analysis was compared with those of full-scale test data reported in Dhar and Moore (2004) to explain some of the local deformations observed during the tests. The study revealed that a local bending governs the strains on some components of the pipe profiles. The mechanism of the local bending was different at the crown (top section) and the springline (mid level section) for the pipes under biaxial loading. The semi-analytical finite element analysis appeared successful in capturing the three-dimensional deformations.

Keywords: Profiled pipe, local bending, axisymmetric analysis, 3-D semi-analytical method, biaxial loading, Fourier harmonics, visco-plastic model

1. Introduction

Buried pipes have been used for water supply and drainage application from the beginnings of modern civilization. Many different pipe products were developed over the last several decades with the purpose to improve economy and performance of the pipes. Profiled-wall pipe was introduced to obtain higher cross-sectional stiffness of the pipe

walls with less utilization of material. A wide variety of wall geometries were developed for this purpose by the pipe manufacturing industry, particularly for thermoplastic pipes. Despite a number of wall-profiles developed for the pipes, the performance limits of those varieties of profiles are not well established yet. The three-dimensional geometries of the profiles led to additional issues requiring consideration during design. Hashash (1991) observed liner (inner wall) buckling and circumferential cracking on the inner walls of a lined corrugated High Density Polyethylene (HDPE) pipe under 100 ft (30.5m) high embankment near Pittsburgh, Pennsylvania, USA. The localized short-wave deformation and inner wall tearing was also found in honey-combed (Tubular profile) HDPE pipe under 40 ft (12.2m) fill at Ohio, USA, (Hurd et al, 1997). A recent study on field performance of HDPE culvert pipes by Gassman et al. (2005) has revealed circumferential cracks, punctures or localized bulges in 36% of 45 profiled HDPE pipes inspected at sites in South Carolina, USA has warranted further study to sufficiently quantify the problems. Moore and Hu (1996) demonstrated earlier from axisymmetric finite element analysis that localized bending on profile components can produce significant tension at the liner-corrugation junction in lined corrugated HDPE pipe. This high tension can be the cause of the circumferential cracking (reported in Hashash 1991, Hurd et al, 1997 and Gassman et al 2005). However, experimental data was not available to verify the local bending reported in Moore and Hu (1996). Laidlaw (1999) measured strains on some profile elements of several lined corrugated HDPE pipes under hoop compression to investigate the local bending experimentally. However, strains on each component (i.e. liner) of those profiles were not measured. Dhar (2002) performed a detailed study to investigate the limit states of different profile-wall pipes using full-scale pipe tests. Based on the study, Dhar and Moore (2001) proposed a model to predict the local buckling on the profile elements. An experimental investigation of local bending and other possible modes of failure of five different profile-wall pipes were reported in Dhar and Moore (2004). This paper presents an analysis of the local bending in two different lined-corrugated profile-wall HDPE pipes using three-dimensional finite element analysis. Figure 1 shows the wall cross-sections (profiles) of the lined corrugated pipe products (also known as twin-wall profiles) considered. Profile 'A' shown in Figure 1(b) possesses a pitch of 101 mm and a corrugation depth of 55.2 mm and Profile 'B' in Figure 1(c) has 80-mm pitch and 58.7 mm corrugation depth. The components of the profiles and their sizes are described in Figure 1. Profile A has a longer span of the liner than Profile B. The twin-wall profiles have annular geometry, where the profile shape is axisymmetric about the pipe axis. Dhar and Moore (2004) demonstrated that a three-dimensional local bending mechanism governs the strains on some components of these profiles. Figure 2 explain a mechanism of the local bending in a lined corrugated profile, which is characterized by less inward movement of the liner than the valley under a radial pressure. Solid lines in the figure represent the original shape of the profile, and the dotted lines show the deflected shape. .

Moore and Hu (1996) revealed that the local bending is a three-dimensional mechanism and it cannot be estimated using conventional 2-D shell theory (that is strain is not linear function of distance from the neutral axis). Full three dimensional modelling of the pipe profile is, therefore, required to analyze the local bending. Moore and Hu (1996) and Moore (1995) investigated the three-dimensional response of lined corrugated pipes using a semi-analytical finite element method. The method is used here to study the three-dimensional behavior of two different thermoplastic pipe profiles. Pipes under two different loading conditions, i.e. axisymmetric stress field and biaxial stress field as shown in Figure 3, were examined. In the axisymmetric stress field a pipe-soil system is subjected to a uniform radial compression as shown in Figure 3(a). Figure 3(b) shows a pipe in a biaxial stress field. A biaxial stress field is expected for a buried pipe laid

horizontally in the ground, where the horizontal ground stress is less than the vertical stress. Axisymmetric analyses were performed to examine the pipes under axisymmetric compression. A semi-analytic (Moore, 1995) method was employed to model the pipes in the biaxial stress field.

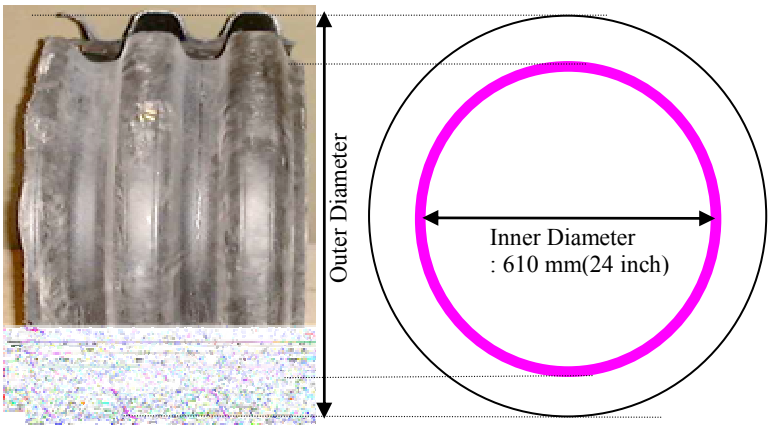

(a) Pipe (Profile A)

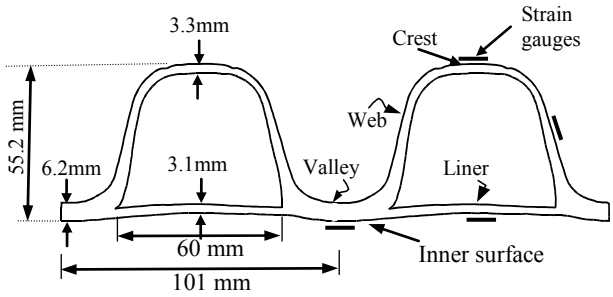

(b) Wall Profile A (liner span = 60 mm)

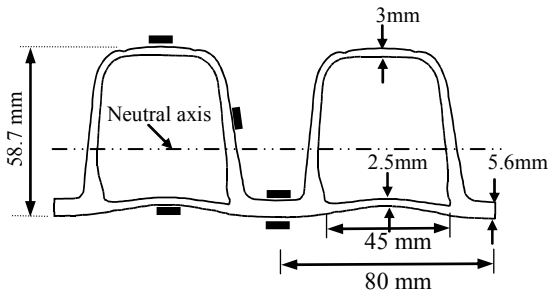

(c) Wall Profile B (liner span = 45 mm)

Fig. 1. Lined corrugated pipe and wall cross-sections (schematic)

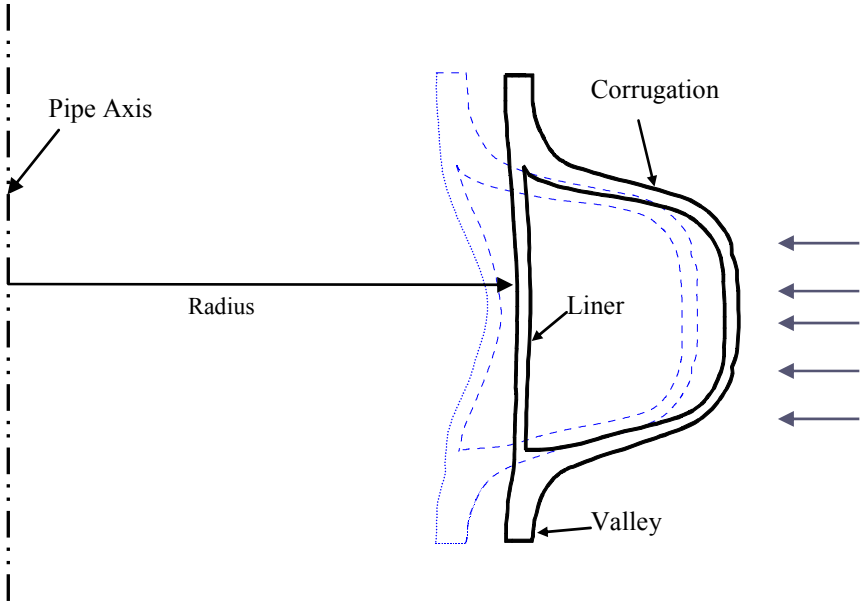

Fig. 2. Mechanism of local bending (after Dhar, 2002)

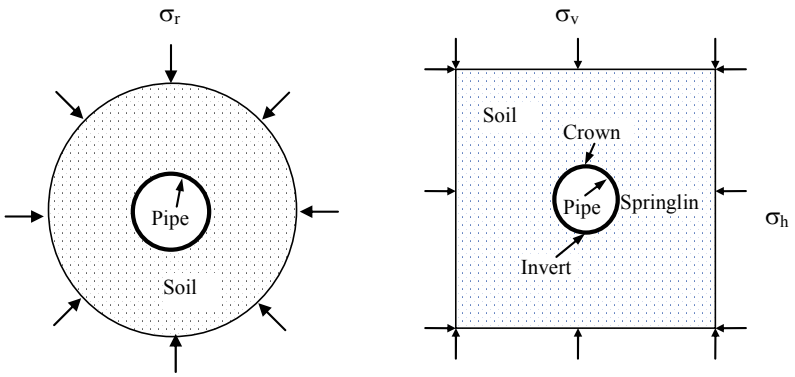

(a) Pipe in axisymmetric stress field (b) Pipe in biaxial stress field

Fig. 3. Pipes in under axisymmetric and biaxial loadings

2. Finite element modeling

2.1 Modeling of pipes under axisymmetric load

Axisymmetric finite element analysis was employed to investigate the response of the pipes under axisymmetric load. Pipes with annular profiles have axisymmetric geometries, and therefore axisymmetric finite element analysis with the finite element mesh defined in the r-z plane can be used to define the problem geometry. Figure 4 depicts a typical finite element mesh used for the annular pipe with lined corrugated profile. The pipes are modeled as being very long, using smooth rigid (axially restrained) boundaries at the top and the bottom of the mesh. A full length of a profile was modeled

since it is not symmetric about any horizontal plane. Six-nodded triangular elements were used to represent both the pipe and the soil in the finite element mesh. Width of the soil zone was chosen as that expected in the Hoop Test Cell for comparison of the results of analyses with the measurements obtained from tests in the Cell. Detail geometry of the finite element mesh used in the axisymmetric analysis will be discussed further in a subsequent section (Section 3.1).

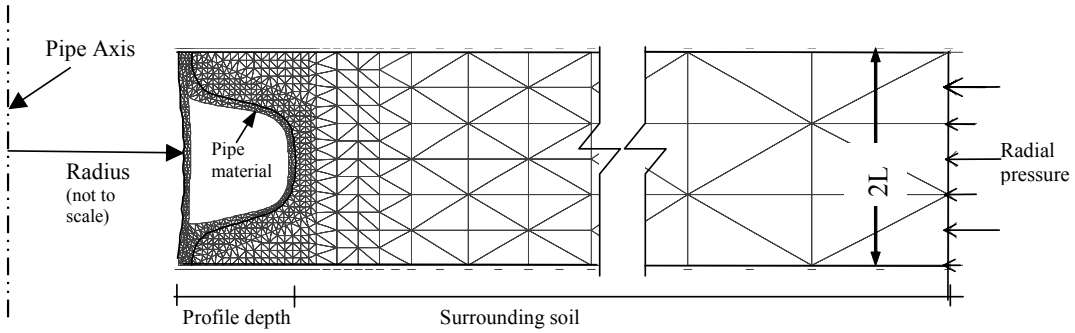

Fig. 4. Finite element mesh for axisymmetric idealization of pipe (Profile A)

2.2 Modeling of pipes under biaxial load

Finite element analysis of axisymmetric structures, such as bins and soils, under non-axisymmetric loads were performed by Ball (1972), Wunderlich et al (1989), Peshkam and Deplak (1993), Rotter and Jumikis (1998), Hong and Teng (2002) and others. Axisymmetric shell elements with circumferential variation of all quantities represented by Fourier series were generally used in the analysis of those structures. Moore (1995) employed axisymmetric continuum elements in the analysis of a profile-wall pipe under biaxial load. The method of Moore (1995) has been used in this study to investigate the behavior of two lined corrugated profiles.

Moore (1995) employed a simplified finite element model in the analysis of pipes with axisymmetric geometry and under biaxial loading. The simplified approach uses a two-dimensional finite element mesh to model the pipe and the surrounding soil in the r, z plane. A Fourier series is used to represent variations around the pipe circumference. The non-axisymmetric loads can be expressed in terms of Fourier harmonics as:

$$f(\theta) = \sum_{n=0}^{\alpha} (F_n^1 Cos\, n\theta + F_n^2 Sinn\theta) \quad (1)$$

where, θ is the angle measured from the crown.

Pipe response to each harmonic coefficient of the load (i.e. F_n^i) is then calculated separately and the combined response is obtained using superposition. Given the dependence on superposition of the semi-analytic method, the analyses are limited to materially and geometrically linear problems.

The features of the harmonic finite element solution are that displacements, strains, and stresses vary along circumference harmonically of same order with the load. For example, a harmonic load, $F_n \cos n\theta$, produces a displacement field given by:

$$(u_r, u_\theta, u_z)^T = \{U_r(n)\cos n\theta, U_\theta(n)\sin n\theta, U_z(n)\cos n\theta\}^T \quad (2)$$

Here u_r, u_θ, u_z are the displacements in r, θ and z direction, and $U_r(n)$, $U_\theta(n)$, $U_z(n)$ are harmonic coefficients of the displacements.

The biaxial geostatic stress can be expressed using radial stress σ and shear stress τ with two harmonic terms of order 0 and 2, respectively as shown in Eqns 3 and 4.

$$\sigma = \frac{\sigma_v + \sigma_h}{2} + \frac{\sigma_v - \sigma_h}{2}\cos 2\theta \quad (3)$$

$$\tau = \frac{\sigma_v - \sigma_h}{2}\sin 2\theta \quad (4)$$

Harmonic coefficients of pipe response, U(n) to each of the two harmonic load coefficients $\frac{\sigma_v + \sigma_h}{2}$ and $\frac{\sigma_v - \sigma_h}{2}$ with n = 0 and n = 2 respectively are obtained from the finite element analysis, which in turn provides the three-dimensional responses, u(n = 0, 2) of the pipe to each of the load components through Eqn 2. The combined response is then obtained from superposition:

$$u = u(0) + u(2) \quad (5)$$

Thus, the simplified three-dimensional finite element procedure of Moore (1995) for biaxial loading conditions uses two-dimensional finite element meshes (similar to Figure 2) for the annular pipes. However, the "outer" radial soil boundary is chosen sufficiently distant (8 to 10 times the radius) to minimize the effect of the boundary on the pipe for analysis of the pipe in the biaxial stress field.

3. Comparison of pipe responses

3.1 Overview

Dhar and Moore (2004) investigated the performance of four different profiles of three types namely, lined corrugated profile, boxed profile and tubular profile using full-scale tests. Two lined corrugated pipes were tested under both biaxial and axisymmetric compressions. In the axisymmetric tests, the pipes were placed upright at the center of a cylindrical cell and backfilled using granular materials. A radial pressure was then applied from the boundary of the cylindrical cell using an air bladder, which was measured using a pressure gauge and a computer controlled Data Acquisition System. Strains on different components of the profiles were also measured to capture the local bending of the components.

Instrumented pipe was laid horizontally in a Biaxial Cell (soil box) which was backfilled using granular material. Several Geokon Earth pressure cells were placed at different locations within the cell to measure horizontal and vertical soil stresses. Two settlement plates were also employed to monitor soil settlements at springline level of the pipe. An air bladder placed on top of the cell was used to apply uniform vertical pressure. The cell pressure was measured using a gauge.

Measurements of pipe responses under both axisymmetric and biaxial loading condition were compared in this study with those obtained from the finite element analysis. Pipes were modeled in the analysis as to simulate the test conditions. Figure 4, shown earlier, reveals a typical finite element mesh used for analysis of a lined corrugated pipes. For simulation of pipe behavior in the axisymmetric loading test, geometry of the FE mesh was used as that of the test cell. The external diameter of the soil region around the pipe corresponds to the inner diameter, 1500mm, of the cylindrical steel Hoop Cell (Dhar and Moore, 2004). This provides a soil ring of width 430 mm surrounding the lined corrugated pipes of 610 mm inner diameter.

In the biaxial tests, pipes were placed horizontally in a rigid-wall soil box. Size of the box is 2m × 2m in plan and 1.6 m height. These allowed a soil thickness approximately equal to pipe diameter on top and on both sides of the pipes. Soil width below the pipe was about half of the pipe diameters. However, an axisymmetric mesh (similar to Figure 4) but with a greater soil thickness was used in the semi-analytical finite element analysis. A study was performed subsequently to examine the effects of this idealization. The measured values of the soil stresses and displacements were used to obtain the parameters for the semi-analytical analysis.

3.2 Material parameters for FE analyses

Pipe Parameters

The use of appropriate constitutive models is necessary to simulate reasonably the physical behavior reasonably using finite element analyses. Thermoplastic material exhibits noticeable time dependent behavior. However, elastic modeling using secant modulus is the most widely used approach for thermoplastic pipe analysis, because of its simplicity. Both a linear elastic model based on the secant modulus and a viscoplastic model of Zhang and Moore (1997) were used in this study to analyze the pipes tested in the axisymmetric cell. Zhang and Moore (1997) developed a viscoplastic model for HDPE material by the framework of Bodner's theory (Bodner and Parton,1972). The theory expresses the second invariant of the deviatoric plastic strain rate as a function of that of stress tensor. For a uniaxial case, the inelastic strain rate can be expressed as:

$$\varepsilon^{\bullet P} = C\left(\frac{\sigma}{X}\right)^{n} \qquad (n \geq 1) \tag{6}$$

where, $\varepsilon^{\bullet P}$ is inelastic strain rate, σ is stress, C is a scale factor, n is a material constant and X is a hardening state variable. The hardening state variable is a function of inelastic work, W^p, inelastic strain rate, $\varepsilon^{\bullet P}$ and was expressed in Zhang and Moore (1997) as:

$$\frac{X_0}{X} = \alpha + \left\{\frac{\beta}{\gamma + W^p}\right\}^{1/2} \tag{7}$$

where,
$$\alpha = d_1 \exp\left\{d_2 \left(\varepsilon^{\bullet P}\right)^{d_3}\right\} \tag{8}$$

Here, X_0, d_1, d_2, d_3, β, γ are constants. Zhang and Moore (1998) determined two sets of viscoplastic model parameters for two HDPE pipe materials obtained from the

manufacturers of the pipes. These parameters were used in the analysis for simulation of axisymmetric tests.

Since the semi-analytic method utilizes the principle of superposition, the linear material properties were needed for analysis of the biaxial loading tests. For the linear model, modulus of elasticity for the high-density polyethylene was taken as the secant modulus corresponding to the time/load for which the simulation was made, based on the data and viscoplastic model of Zhang and Moore (1997). Thus, the secant modulus for simulation of pipe response corresponding to a cell pressure was estimated using the pressure and the time to reach it, assuming a constant rate of loading. For the pipe response at the maximum cell pressure in the biaxial tests, pipe modulus was estimated to be 450 MPa, representing a value for 6 hours, i.e. the time required to reach the pressure. Parameters used for pipe materials are summarized in Table 1.

Soil Parameters

As discussed earlier, the analysis of the pipe in the biaxial stress field involved the principle of superposition and therefore a linear elastic analysis was performed. Elastic secant moduli for the soil used in the biaxial test were determined from the measurements of vertical stress and average vertical strain in a column of soil adjacent to the pipes (Dhar et al. 2004). The secant modulus thus obtained was 6.4 MPa, representing a value for the loose sand. No compaction was used during placement of soil in the biaxial tests (see also Dhar and Moore 2004). The Poisson's ratio for the soil was calculated from the lateral earth pressure co-efficient, K as $\nu = K/(1+K)$ to ensure the lateral earth pressures for zero lateral strain as those were expected in the tests. The horizontal and vertical soil stresses measured during the tests were used to calculate the co-efficient of lateral earth pressure. The lateral earth pressure co-efficient thus calculated was 0.5.

Stresses and deformations of the soil were not measured during the hoop cell tests. Soil parameters used for the analysis of the hoop test were those reported by Zhang and Moore (1998), who undertook an analysis of a pipe tested in the same backfill. However, the degree of compaction achieved in each hoop compression test was variable, since compaction was difficult to control in the narrow space between the pipe and the test cell wall in the Hoop Cell (Dhar and Moore, 2004). The soil in the Hoop Cell was compacted using a 10 lb tamper to obtain a higher density according to Dhar and Moor (2004). Therefore, a higher modulus is expected for the soil in the Hoop Cell.

An elasto-plastic soil model was used for the analysis of the pipe in the axisymmetric stress field. The Mohr-Coulomb model was used for the elasto-plastic behavior of the soil. The angle of internal friction for the model was selected to be $\phi = 36^{o}$, based on which the material was classified as "SW85" by Selig (1990). Table 2 summarizes all the soil parameters used in the finite element analyses of the tests. Angle of dilation was used as same as the angle of internal friction. However, an analysis was also performed using a smaller dilation angle (i.e. 13^{o}, which is a typical value for granular material; Skempton 1984), which showed no significant differences (less than 1% deviation in deformation) in the finite element results for these test cases.

Table 1
Pipe parameters used in the FE analysis

Material/model	Parameter
HDPE pipe (linear model)	Modulus, E= 450 MPa (secant modulus at maximum load) Poisson's ratio, $\nu = 0.46$
HDPE pipe (VP model-1) Zhang and Moore (1998)	E = 1350 MPa, $\nu = 0.46$, C=0.01, n=8.0 $\gamma = 10^{-4}$ MPa, $\beta = 7.744\times 10^{-5}$ MPa, $d_1 = 1.055\times10^{-3}$, $d_2 = 3.829$, $d_3 = 2.55\times10^{-2}$
HDPE pipe (VP model-2) Zhang and Moore (1998)	E = 1450 MPa, $\nu = 0.46$, C=0.01, n=8.0 $\gamma = 10^{-4}$ MPa, $\beta = 7.056\times 10^{-5}$ MPa, $d_1 = 1.042\times10^{-3}$, $d_2 = 3.829$, $d_3 = 2.547\times10^{-2}$

Table 2
Soil parameters for FE analyses

Analysis type	Parameters
Axisymmetric	Modulus, E= 30 MPa Poisson's ratio, $\nu = 0.2$ Cohesion, C=0 Angle of internal friction, $\phi = 36^o$
3-D semi-analytical	Modulus, E = 6.4 MPa Poisson's ratio, $\nu = 0.33$

3.3 Profile responses under axisymmetric load

Figure 5 plots the measurements of pipe deflection for a lined corrugated pipe (Profile B) together with the finite element calculations. The figure shows that the analysis of using the viscoplastic model matched the measurements of pipe deflection well. The rate of loading of the analysis was used as same as that applied during the tests (i.e., 1.39 kPa/min) for the time dependent simulation. The other profile with relatively a longer liner span (Profile A) also showed similar comparison, however, not included in this paper for brevity. Since there is only a thin ring of soil surrounding the pipe in the hoop cell, the stiffness of pipe is particularly important. The effect of pipe stiffness is expected to be more for the pipe in the Hoop Cell than for the same pipe in the field where the pipe lies within an extensive zone of backfill and native soil. True viscoplastic parameters of the pipe material for this test were available in Zhang and Moore (1998). Thus the viscoplastic model simulates the non-linear time-dependent behavior of the HDPE material very effectively.

Experimental measurements and calculated values of hoop strain on the interior and exterior surfaces of the profile are compared in Figures 6 and 7 respectively. Strains are plotted as a function of the radial pressure applied at the outer boundary of soil. The

finite element method appears to calculate reasonably the hoop strains on both the interior and exterior surfaces of the pipe. Calculated strains on the liner are less than those on the valleys (Figure 6), just as the measured values were found to be, the analysis capturing the local bending that occurs in the liner, where it spans between corrugation valleys. However, the measurements show stabilization of liner strains at high cell pressure in Figure 6, while the analysis continues to predict strain increases with the increases of cell pressures. Ripples were evident on the liner at high cell pressures during the experiment indicating that the element buckled locally. Due to the development of local buckling the liner losses its capacity to carry further load, which is the reason for the strain stabilization (Dhar and Moore, 2001). The local buckling is a geometrically nonlinear phenomenon which could not be captured using the linear analysis presented here. A geometrical nonlinear analysis as those of Teng and Hong (1998), Rotter and Jumikis (1998) and Hong and Teng (2002) is required to investigate the local buckling. Nonlinear relationships between measured strain and cell pressure are also seen on both the web and the crest of the exterior walls (Figure 7), once again as a result of the local buckling of these elements. Strains on these exterior elements may also be influenced by the local soil support. However, Figure 7 indicates that the finite element model appears to provide a conservative estimate of hoop strains on these exterior elements.

Distributions of calculated and measured hoop strains along the interior surface of the profile are plotted in Figure 8 at a radial earth pressure of 150 kPa. Strains on both of the profiles are shown in the figures. The magnitude of the measured hoop strain at the mid-liner is somewhat lower than the calculated value, while calculated valley strain matches the measurements well. It is evident from the figures that the hoop strains are not uniform along the inner surface of the lined corrugated profiles (even though the distance of the inner wall from the neutral axis of the profile is almost the same). The local bending results in compressive hoop strains that reduce from maxima at the valleys to minima at the mid position, where the liner spans between the valleys (Figure 8). Analysis shows the liner strain as about 70% of the valley strain for Profile B (having shorter liner span), while the measurment showed the strain as 65%. The ratio of the liner to valley strain for Profile A was 0.50 (measured 0.60). Thus the ratio of the liner to valley strain is less for profile A, indicating greater effect of local bending on this profile with longer liner.

Figure 9 shows axial strains on various elements of the profile. The differences in the axial strains on the inner and the outer surface of the valley are associated with longitudinal bending. The longitudinal bending on the exterior elements may be influenced by local interaction with the soil. However, the analysis appears to provide reasonable estimates of these strains.

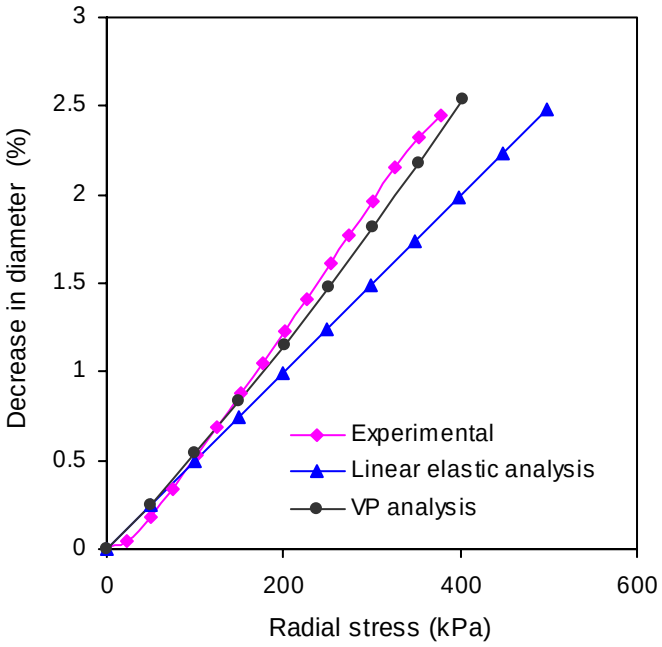

Fig. 5. Deflections of pipe under axisymmetric loading (Profile B)

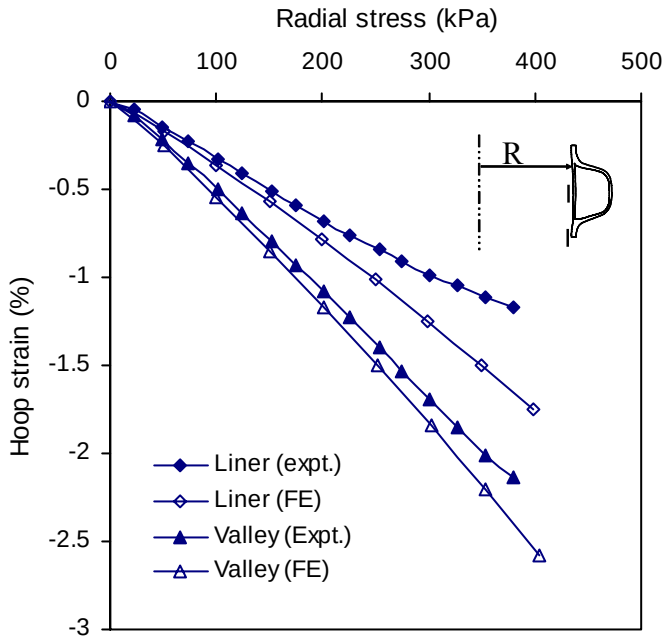

Fig. 6. Comparison of hoop strain on the inner walls (Profile B)
(R not to scale)

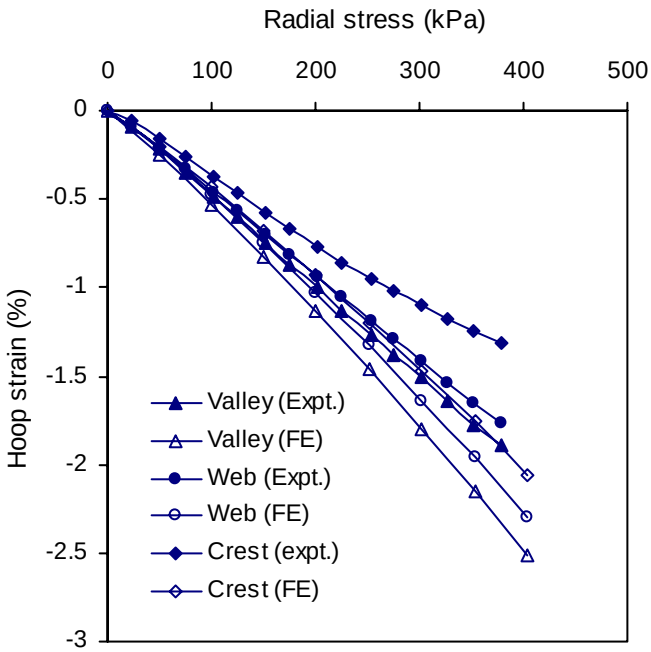

Fig. 7. Comparison of hoop strain on the exterior walls (Profile B)

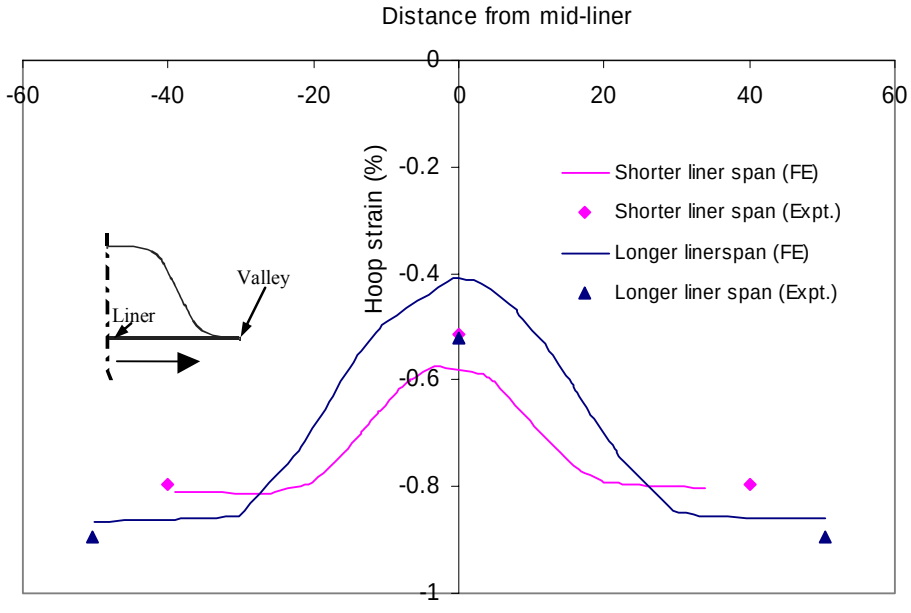

Fig. 8. Distribution of hoop strain on inner wall (at 150 kPa of radial pressure)

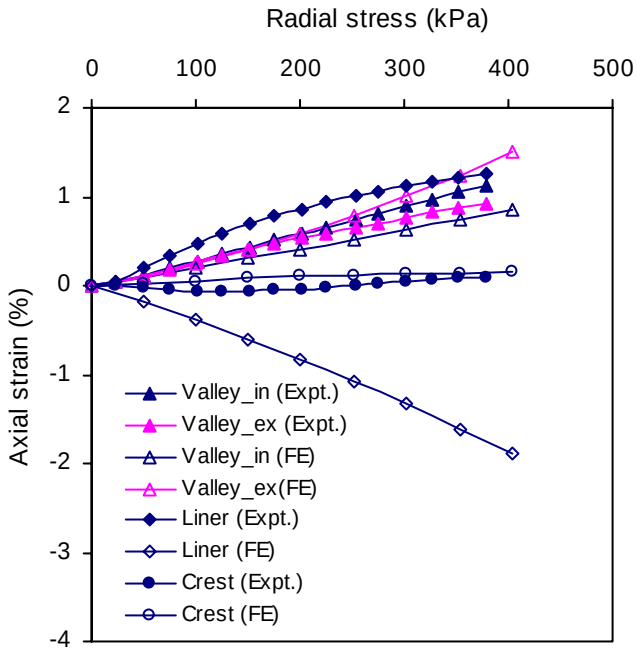

Fig. 9. Comparison of axial strains under axisymmetric loading (Profile B)

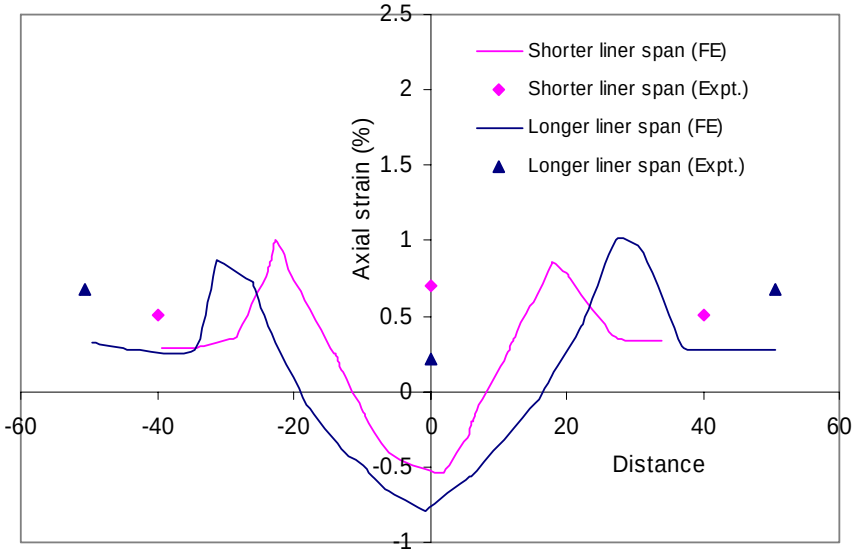

Fig. 10. Axial strain distribution in inner wall (at 150 kPa of radial pressure)

The analysis predicts the compressive strain on the inner surface at the mid-point of the liner, however, axial tension was measured during the tests. This discrepancy likely resulted, because plane strain conditions may not be achieved in the test cell, though plane strain condition was assumed in the FE analysis. The corrugated element has little axial stiffness, so failure to develop significant axial constraint may have little effect on the local stress or strain. The liner, however, forms a continuous cylindrical shell that has substantial axial stiffness. Axial strains will develop in the liner in the absence of full axial restraint on the pipe, though this is associated with axial stretching not local bending. The measurements of axial strain on the liner show high tensions in Figure 9. Only one strain gauge for measuring axial strain on the liner was working during this test (Dhar, 2002), therefore, the data could not be verified in the same manner as the other strain measurements, where several strain gauge readings were obtained.

Distribution of axial strain along the interior surface of the profile is shown in Figure 10 at the same radial pressure of 150 kPa. The finite element analysis indicates that there is a local increase in tensile axial strain at the liner-corrugation junctions of both profiles (Figure 10). No measurements of strains were made because of the difficulty of attaching gauges directly at this position. The axial tensile strain at the liner-corrugation junction caused by the local bending of the profile, if high enough, may cause circumferential cracking as observed in Hashash (1990).

3.4 Profile response under biaxial load

The three-dimensional semi-analytic method of Moore (1995) is used to analyze the pipe under biaxial loading tests. The finite element model approximates the pipes as buried in an infinite region of elastic ground. A study was undertaken to locate the external soil boundary at a sufficient distance from the pipe so that it does not affect pipe behavior. Two-dimensional finite element analysis with actual modelling of the test cell was subsequently performed to verify the assumption of infinite ground in the three-dimensional analysis. The two-dimensional analysis of the pipes used conventional structural theory based on section properties; area, A and second moment of area, I. Results of the two-dimensional and the three-dimensional analysis of the same pipe with the same linear material parameters were compared in Figure 11. Pipe responses are plotted against the pressure applied on top of the soil in the figure. The two analyses provided similar values of changes in pipe diameter, Figure 11, confirming that the 3D Fourier analysis provides a reasonable simulation of pipe deflection under geostatic stresses.

This section of the paper focuses on the comparison of pipe responses measured at the crown (top section) and the springline (mid-level section) of pipe with those from the finite element analyses. No comparisons were made with strain values obtained at the inverts of the pipe specimens, since invert (bottom section) strains may be greatly influenced by the proximity to the boundary and a low stiff soil zone under the pipe haunches.

Figure 12 compares the calculated values of change in pipe diameter (using 3-D analysis) under biaxial load with the measurements for both of the pipes. D_h and D_v in Figure 12 indicate changes in horizontal and vertical pipe diameters respectively. Deflections are plotted as a function of the vertical cell pressure applied at the surface of the biaxial cell (this vertical pressure is equivalent to the overburden pressure the soil-pipe system would experience when deeply buried in an embankment). Triangles represent the pipe

with shorter liner span (Profile B) and circles represent for the pipe with longer liner span (Profile A). In the FE analysis, soil and pipe modulus (secant modulus) corresponding to the maximum vertical cell pressure was used. Therefore, estimated responses at the maximum pressure would be compared with the measurements. Estimated deflections at the maximum vertical pressure in Figure 12 are reasonably close to the measurements. Similar results were obtained using the two-dimensional analysis with a linear elastic soil model using secant modulus (Dhar et al, 2004). Assumption of linear soil model resulted in calculated response to be stiff relative to the measurements in Figure 12. While nonlinear elasto-plastic soil modeling furnishes a better two-dimensional simulation, Dhar et al. (2004), this non-linear behavior cannot be considered in the semi-analytic finite element analysis, since it is based on superposition of the pipe responses to each of the two different Fourier harmonic coefficients of applied earth pressure.

Comparison of circumferential strains at the springline and the crown are shown (Figures 13 and 14). Figure 13a shows the strains on the interior surface on the liner and valley of both of the pipe profiles. Measurements show a change in the curvature of the stress-strain curve at low pressure for the pipe with shorter liner span (i.e. Figure 13), which corresponds to a re-compression. The test had to be re-run because the air bladder used in the test failed during the first run at a cell pressure of 75 kPa. The same test was re-loaded using a new bladder, Dhar and Moore (2004). Figure 13 shows that the 3-D analysis provides upper bound estimates of the hoop strain at the springline on both the interior and exterior surfaces of the pipes. The strains on the exterior elements of the profile with longer liner span (Profile A) are not included in Figure 13(b) to avoid awkwardness. The difference of strains between the interior and the exterior surfaces of the corrugation valley is not great, because high hoop thrust governs the strain at the springline rather than the bending. The finite element procedure overestimates the strains, perhaps due to not considering the material and geometric non-linearity. Two-dimensional analysis with a non-linear soil model (Janbu 1963) was found to provide rational estimates of a hoop strain on both the valley and the crest of the pipe, Dhar et al. (2004).

At the crown, the semi-analytic finite element method provides rational estimates of the strain on both the liner and the valley (Figure 14). However, the non-linear development of wall and crest strain with overburden pressure was not calculated well; again. The method neglects the influence of the local buckling that has developed in these profile elements.

As in the hoop tests, local bending caused the circumferential strain on the liner to be a fraction of the valley strain. This is seen in the semi-analytic finite element calculations, as well as in the measurements (Figure 13a). For the pipe with short liner span (Profile B), the semi-analytic finite element model calculates the liner strains as to be 65% and 85% of the valley strains respectively at the springline and at the crown for the profile. The measured values for the corresponding strains were 30% and 80% respectively. Thus, the ratio at the springline is less than the ratio at the crown in both the calculation and the measurement, indicating different mechanism of local bending at these two positions. Axisymmetric finite element analysis for the profile gives the liner strain as to be 70% of the valley strain. The liner strain in the axisymmetric test was 65% of the valley strain (Dhar and Moore, 2004). Thus, the ratio of liner to valley strain appears to depend on the circumferential bending of the section. The springline of the pipe is

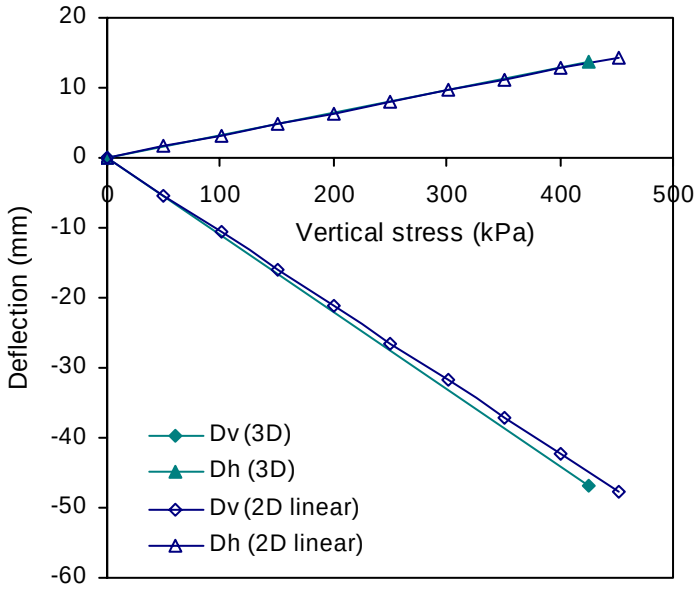

Fig. 11. Comparison of deflections from 2-D and 3-D FE analysis

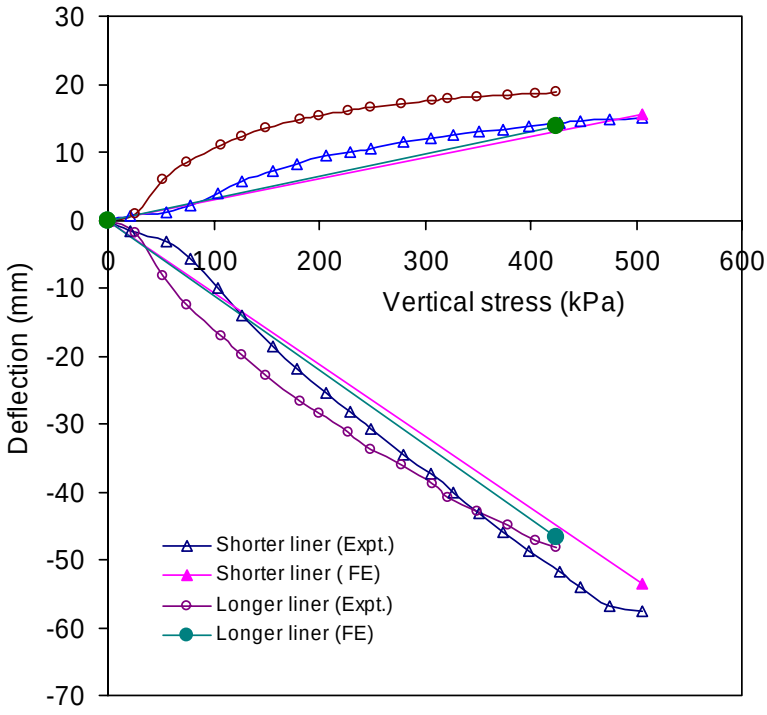

Fig. 12. Deflections of pipes under biaxial loading (Profile B)

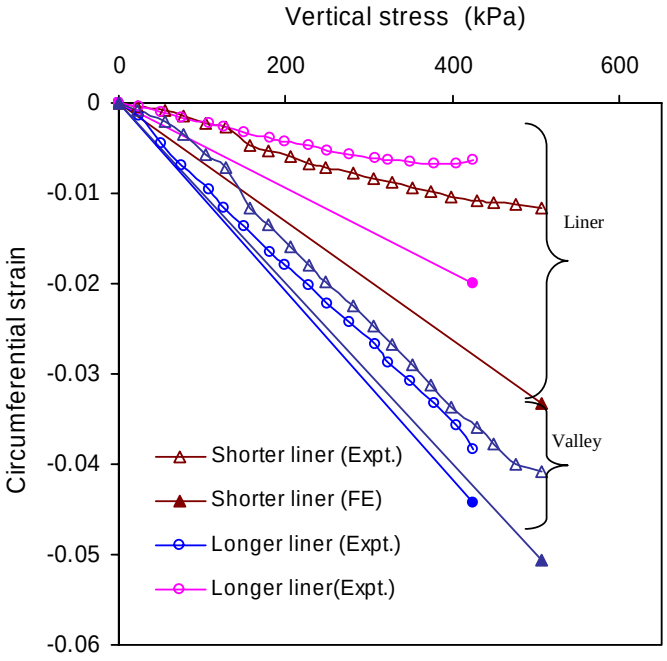

(a) Strain on the interior wall

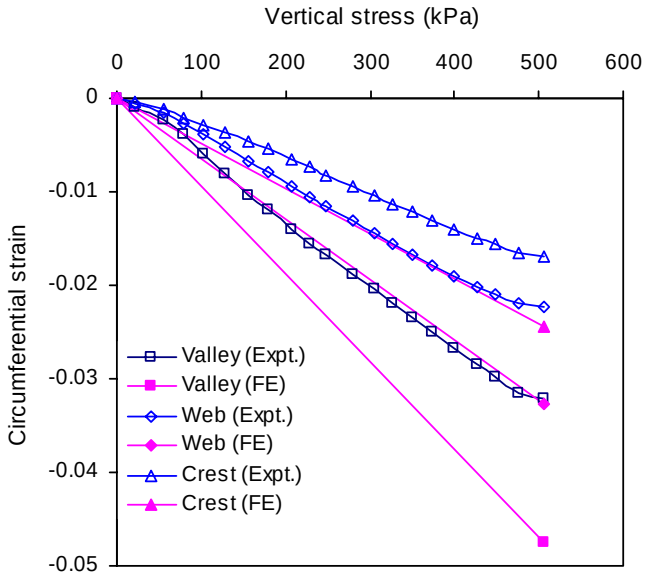

(b) Strain on the exterior wall

Fig. 13. Circumferential strains at the springline (Profile B)

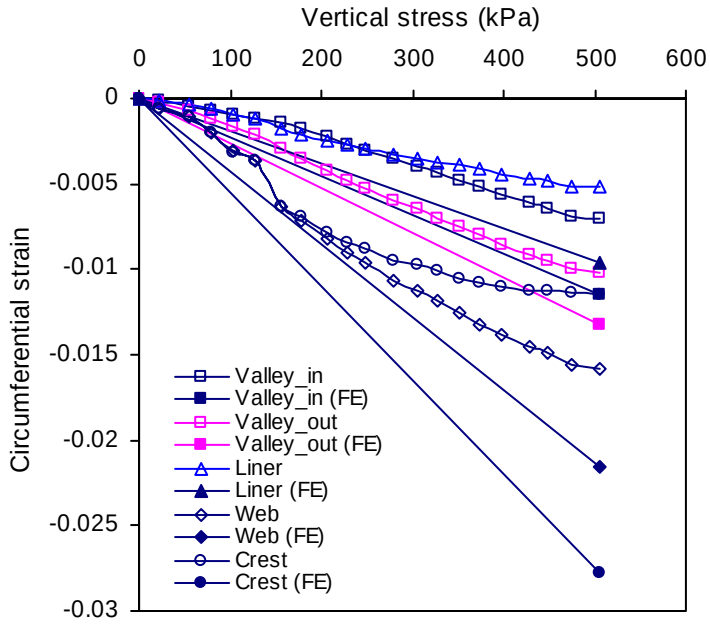

Fig. 14. Circumferential strains at the crown (Profile B)

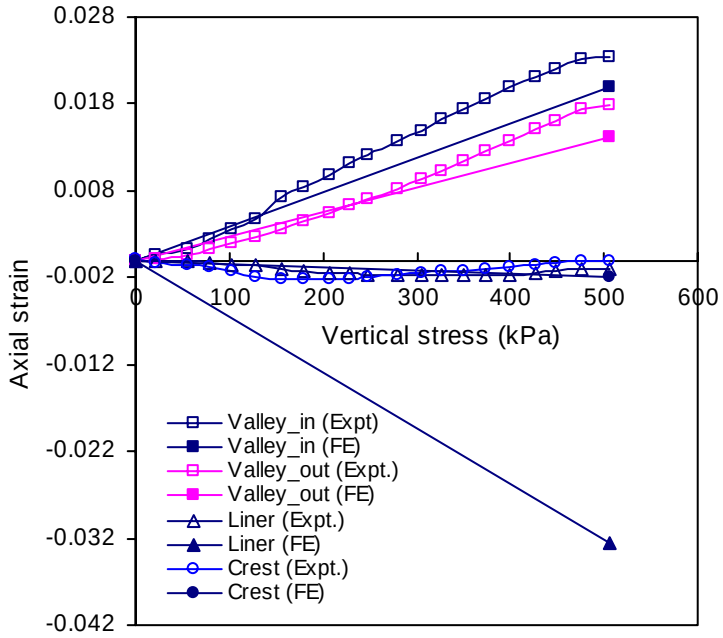

Fig. 15. Axial strains in lined corrugated profile (at springline)

subjected to positive bending (compression inward) and the crown to negative bending (compression outward) for a pipe horizontally laid in the ground. The section under positive bending (the springline) has a smaller proportion of the valley strain developing on the liner than the sections with no bending (pure hoop compression) or with negative

bending (the crown). The ratios of liner to valley strains for Profile A (having longer liner span) was also less at the springline than that at the crown. The ratios were 0.45 (measured 0.20) and 0.55 (measured 0.30) at the springline and crown respectively. It is also evident that the ratios are always less for the pipe with longer liner span, indicating greater effects of local bending on the longer liner.

Figure 13 shows comparisons between calculated and measured values of axial strain in the elements of the profile. Only the springline strains are shown in Figure 13, since both crown and the springline showed similar comparison. Figure 13 shows that strain calculations are reasonable, except those for the liner. Very high axial compressive strain was calculated on the liner, while measurements showed minimal axial compression at the springline. This is likely due to the fact that true plane strain condition could not be achieved during the tests.

4. Summary and conclusion

Three-dimensional response of two lined corrugated profiled HDPE pipes was examined in this paper using finite element analysis. The pipe profiles were modeled explicitly using the profile geometry recorded from various test specimens. Results of the analysis were compared with the measurements from full-scale laboratory tests (Dhar and Moore 2004).

The study revealed that local bending governs the strains on the components of lined corrugated profile. The liner of the two lined-corrugated profiles considered here was subjected to significant local bending. Due to the bending, circumferential (hoop) strain on the liner was less than that at the valley, even though the points were located at the same distance from the neutral axis of the profile. The localized bending on the liner was found to depend on the span of the liner (the distance it stretches between corrugation valleys), with greater effects on the liner with longer span.

For a pipe buried horizontally in the ground, the mechanism of the local bending was different at the crown and the springline. The ratio of the liner strain to valley strain was 0.65 (measured 0.3) and 0.85 (measured 0.8) at the springline and crown respective for the pipe Profile B. The ratio for the same profile under axisymmetric loading was 0.7 (measured 0.65). For the other pipe (Profile A), the ratios were 0.45 (measured 0.2) and 0.55 (measured 0.3) respectively at the crown and springline. A significant axial tension may develop on the profile element due to the localized bending.

It was also revealed that a semi-analytical finite element analysis can effectively be used to capture the local bending for a pipe in a realistic (biaxial) stress field. The axisymmetric finite element analysis was successfully used to model the response of the pipe profiles in the axisymmetric stress field. The study resulted in a better understanding of the three-dimensional behavior of the twin-wall profiled pipe.

Notations

θ	Angular distance measured from crown
σ	Radial stress
τ	Shear stress
σ_v	Vertical stress
σ_h	Horizontal stress

D	Diameter of pipe
D_h	Change in horizontal pipe diameter
D_v	Change in vertical pipe diameter
u_r, u_θ, u_z	Radial, tangential and axial displacements
U_r, U_θ, U_z	Harmonic coefficients of displacements
E	Modulus of elasticity
υ	Poisson's ratio
C	Cohesion
φ	Angle of internal friction
C, n, γ, β, d_1, d_2, d_3	Viscoplastic parameters

References

Ball, R.E. (1972), A program for the static and dynamic analysis of arbitrarily loaded shells of revolution, Computers and Structures, 2, 141–62.

Bodner, S.R. and Parton, Y. (1972), A large deformation elastic-viscoplastic analysis of a thick-walled spherical shell, Journal of Applied Mechanics, 42, 385-389.

Dhar, A. (2002), "Limit states of profiled thermoplastic pipes under deep burial", Ph.D. thesis, Department of Civil and Environmental Engineering, The University of Western Ontario, London, Canada.

Dhar, A.S. and Moore, I.D. (2001), Liner buckling in profiled polyethylene pipes, Geosynthetics International, 8, 193-216.

Dhar, A.S. and Moore, I.D. (2004), Laboratory investigation of local bending in profiled thermoplastic pipes, Advances in Structural Engineering-An International Journal, 7, 201-215.

Dhar, A.S., Moore, I.D. and McGrath, T.J. (2004), Thermoplastic culvert deformation and strain: evaluation using two-dimensional analyses, ASCE Journal of Geotechnical & Geoenvironmental Engineering, 130, 199-208.

Gassman, S. L., Schroeder A. J., A. and Ray R. P. (2005), Field performance of high density polyethylene culvert pipe, ASCE Journal of Transportation Engineering, 131, 160-167.

Hashash, N.M.A., (1991), "Design and Analysis of Deeply Buried Polyethylene Drainage Pipes" Ph.D. Thesis, Department of Civil Engineering, The University of Massachusetts, Amherst, Massachusetts, USA.

Hong T. and Teng J.G. (2002), Non-linear analysis of shells of revolution under arbitrary loads", Computers and Structures, 80, 1547-1568.

Hurd, J.O., Sargand, S.M, and Masada, T. (1997), Performance of large diameter HC-HDPE pipe under highway Embankment in Ohio, Paper no. 970894, 76th Annual Meeting, Transportation Research Board, Washington, D.C.

Janbu, N. (1963), Soil compressibility as determined by odometer and triaxial tests, Proceedings of the European Conference on Soil Mechanics and Foundation Engineering, Wiesbaden, 1, 19-25.

Laidlaw, T.C. (1999), "Influence of Local Support on Corrugated HDPE Pipe", M.E.Sc. Thesis, Department of Civil and Environmental Engineering, The University of Western Ontario, London, ON, Canada.

Moore, I.D. and Hu, F. (1996), Linear viscoelastic modelling of profiled high density polyethylene pipe, Canadian Journal of Civil Eng., 23, 395-407.

Moore, I.D. (1995), Three dimensional response of deeply buried profiled polyethylene pipe, Transportation Research Record 1514, 49-58.

Peshkam, V. and Delpak, R. (1993), A variational approach to geometrically non-linear analysis of axisymmetrically loaded rotational shells: II. Finite element application, Computers and Structures, 46, 1–11.

Rotter, J.M. and Jumikis, P.T. (1998), Nonlinear Strain-displacement Relations for thin shells of Revolution, Research Report R563, School of Civil And Mining Engineering, University of Sydney, Australia.

Selig, E.T, (1990), "Soil Properties for Plastic Pipe Installations", ASTM Special Technical Publication 1093, Buried Plastic Pipe Technology, W. Conshohocken, Pa. 141-158.

Skempton, A. (1984), "Effective stress in soils, concrete and rocks", Selected Papers on Soil Mechanics by Skemption, A.T. Telford, London, pp. 4-16.

Teng, J.G. and Hong, T.(1998), Non linear thin shell theories for numerical buckling prediction, Thin-walled structures , 31, 89-115.

Wunderlich W, Obrecht H, Springer H, Lu Z. (1989), A semianalytical approach to the nonlinear analysis of shells of revolution. In: Noor AK, Belytschko T, Sino JC, editors. Analytical and computational models for shell. NY: ASME, 505–36.

Zhang, C. and Moore, I.D. (1997), Nonlinear mechanical response of high density polyethylene. part II: uniaxial constitutive modeling, Polymer Engineering and Science, 37, 414-420.

Zhang, C. and Moore, I.D. (1998), Nonlinear finite element analysis for thermoplastic pipes", Transportation Research Record No. 1624, Journal of Transportation Research Board, 225-230.